

On Parameter Estimation of Flexible Space Manipulator Systems

Olga-Orsalia Christidi-Loumpasefski, *Student Member, IEEE*, Kostas Nanos, and Evangelos Papadopoulos, *Fellow, IEEE*

Abstract. Space manipulator systems in orbit are subject to link flexibilities since they are designed to be lightweight and long reaching. Often, their joints are driven by harmonic gear-motor units, which introduce joint flexibility. Both of these types of flexibility may cause structural vibrations. To improve endpoint tracking, advanced control strategies that benefit from the knowledge of system parameters, including those describing link and joint flexibilities, are required. In this paper, first, the equations of motion of space manipulator systems whose manipulators are subject to both link and joint flexibilities are derived. Then, a parameter estimation method is developed, based on the energy balance during the motion of a flexible space manipulator. The method estimates all system parameters including those that describe both link and joint flexibilities and can reconstruct the system full dynamics required for the application of advanced control strategies. The method, developed for spatial systems, is illustrated by a planar example.

I. INTRODUCTION

A challenge in the design of space robotic manipulators, see Fig. 1, is to use light materials, suitable for typical on orbit tasks. Lightweight structures are expected to improve their payload-to-arm mass ratio. A drawback of such lightweight space manipulators is the increased link structural flexibility. In addition to these flexibilities, space manipulators also are subject to joint flexibilities. Such flexibilities arise when motion transmission elements such as harmonic drives, transmission belts and long shafts are used. Both of these types of flexibilities cause vibrations, which are profound when manipulating large payloads; if neglected in the control design, they may even result in instabilities [1]. Therefore, advanced control strategies are required, which however, need knowledge of system parameters.

To estimate the flexible joint parameters of a space manipulator, the development of a simplified coplanar model of the flexible joint was proposed, [2]. The joint stiffness and damping were found by applying an impact force on the system and studying the resulting response. More recently, an estimation method based on the system energy balance has been developed, [3]. This method can be used for estimating

the parameters of flexible-joint free-floating space manipulator systems (SMS), since it tolerates measurement noise and yields all parameters required for the system dynamics and the design of advanced controllers for space applications such as trajectory following, [1]. However, link flexibilities have not been considered in these studies.

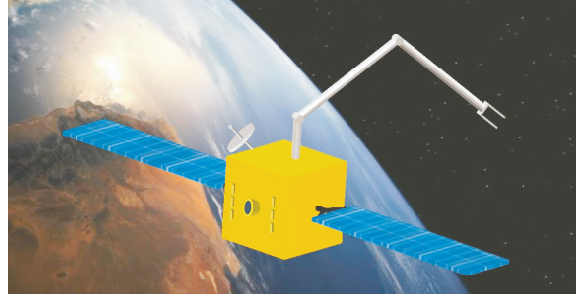


Fig. 1. A flexible space manipulator system.

Regarding the estimation of flexible link parameters, in the literature, fixed-base manipulators are mostly considered. A fast online closed-loop continuous-time estimator of the natural frequency of a single flexible-link has been proposed, [4]. The proposed methodology requires the measurements of the angular position of the motor and the coupling torque. To estimate physical parameters such as Young modulus and the mass or the length of the segments of a fixed-base flexible link manipulator, a linear parameter-varying descriptor state-space structure of the manipulator has been developed in [5]. To tolerate measurement noise, a method based on energy balance has been developed to estimate the physical parameters of a flexible link manipulator, [6]. An experimental procedure has been presented that yields the system stiffness, mass, and damping parameters of an industrial manipulator based on a modal analysis concept, for use in an accurate model for the control system [7]. The observer/Kalman filter identification and the eigensystem realization algorithm have been applied to identify the structural modal parameters of solar panels mounted on satellites, [8]. In our previous work [3] all inertial and flexible joint parameters of a SMS were estimated. Although this is an important realization, additional parameters are required to describe the effects of flexible links. However, parameter estimation for SMSs, subject to both link and joint flexibilities, is a challenging problem. To the best of our knowledge, no parameter estimation study considering both link and joint flexibilities of SMSs exists.

In this paper, the energy balance method is applied in order to estimate link flexibility parameters in addition to all system inertial and joint flexibility parameters of a SMS. These parameters can reconstruct the system full dynamics as required by advanced control strategies. The proposed

O.-O. Christidi-Loumpasefski was supported by an Onassis Foundation Scholarship.

Kostas Nanos' research is co-financed by Greece and the European Union (European Social Fund-ESF) through the Operational Programme «Human Resources Development, Education and Lifelong Learning» in the context of the project «Reinforcement of Postdoctoral Researchers - 2nd Cycle» (MIS-5033021), implemented by the State Scholarships Foundation (IKY).

O.-O. Christidi-Loumpasefski, Kostas Nanos & Evangelos Papadopoulos are with the School of Mechanical Engineering, National Technical University of Athens, Greece (ph.: +30-210-772-1440; e-mail: {olgaioumpasefski, nanos.kostas}@gmail.com, egpapado@central.ntua.gr).

method is tolerant to noise since it does not require acceleration measurements. The method, developed for spatial systems, is illustrated by a planar example.

II. FLEXIBLE SPACE MANIPULATOR SYSTEMS MODELING

An on-orbit SMS can be considered as a central rigid body (spacecraft) with an N -link manipulator with flexible joints and links mounted on it.

A. Flexible Joint Model

Each joint is actuated with a torque τ applied by a DC brushless motor equipped with a harmonic drive (reducer). Due to the use of these drives, the joints are considered to be flexible. To derive the flexible joint model, the following assumptions are made. First, joint deflections are considered small enough so that they can be described by a torsion spring of constant stiffness k and by a damping element of constant damping b , see Fig. 2. In the presence of reduction gears of reduction ratio n , the joint deflection is lumped after the gearbox, while the actuator rotor is modeled as a rigid body, with its Center of Mass (CM) on the rotation axis. The stator of joint's i motor is mounted on link $i-1$ while its rotor moves link i with its rotation axis aligned with the i -th joint. To derive the dynamic model of a flexible joint, both the link-side and gear motor-side angular position q and θ_m , respectively, are required; see Fig. 2, [1].

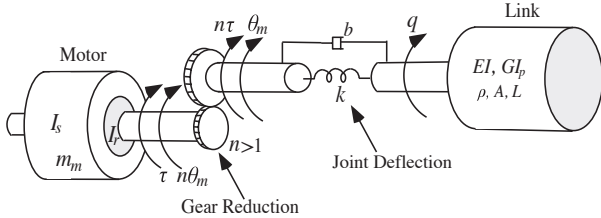


Fig. 2. Physical model of a flexible joint and a flexible link.

B. Flexible Link Model

To describe the flexible link deformation, each link is modeled as a Euler-Bernoulli beam with uniform density ρ , uniform cross-section A , flexural rigidity EI , torsional rigidity GI_p and constant link length L , see Fig. 2. All sections experience a linear and angular deformation in three axes, modeled by traction, bending and torsion, [9].

In deriving the flexible link model, the Finite Element Method (FEM) is employed. In this method, the continuous flexible links are divided in a number of finite elements. The displacement at some link point is expressed in terms of *nodal* displacements [10]. Polynomial interpolation functions are defined in each element.

Here, it is considered that each element has two nodes. The *local* nodal displacements $\mathbf{q}_f^{(i)}$ of element j of link i are

$$\mathbf{q}_{f_j}^{(i)} = \begin{bmatrix} u_{1j}^{(i)T} & \theta_{1j}^{(i)T} & u_{2j}^{(i)T} & \theta_{2j}^{(i)T} \end{bmatrix}^T, \quad i=1, \dots, N \quad (1)$$

where $u_{kj}^{(i)}$ and $\theta_{kj}^{(i)}$ ($k=1,2$) are the *local* translations and rotations of node k of element j of link i along and about the x_i, y_i, z_i axes, see Fig. 4, respectively

$$u_{kj}^{(i)} = [u_{x_{kj}}^{(i)} \ u_{y_{kj}}^{(i)} \ u_{z_{kj}}^{(i)}]^T, \quad \theta_{kj}^{(i)} = [\theta_{x_{kj}}^{(i)} \ \theta_{y_{kj}}^{(i)} \ \theta_{z_{kj}}^{(i)}]^T, \quad k=1,2 \quad (2)$$

To derive the energy equation of flexible links in Section IV. A. (see Eq. (11)), the displacement fields along the beam elements of links must be defined. The $\bar{u}_{y_j}^{(i)}(x_j^{(i)})$ and $\bar{u}_{z_j}^{(i)}(x_j^{(i)})$ are the displacement fields due to bending along the y_i and z_i axes, respectively, $\bar{\theta}_{y_j}^{(i)}(x_j^{(i)})$ and $\bar{\theta}_{z_j}^{(i)}(x_j^{(i)})$ are the corresponding slopes, $\bar{u}_{x_j}^{(i)}(x_j^{(i)})$ and $\bar{\theta}_{x_j}^{(i)}(x_j^{(i)})$ are the displacement fields due to traction and torsion respectively, along and about the x_i axis. Cubic polynomials are used to describe $\bar{u}_{y_j}^{(i)}(x_j^{(i)})$ and $\bar{u}_{z_j}^{(i)}(x_j^{(i)})$, while linear interpolations are used for both $\bar{u}_{x_j}^{(i)}(x_j^{(i)})$ and $\bar{\theta}_{x_j}^{(i)}(x_j^{(i)})$, [11].

The coefficients of the polynomials associated with the description of the displacement fields along the j -th element of link i are obtained by applying the displacement fields, at nodal points, i.e. $x_j^{(i)}=0$ and $x_j^{(i)}=L_j^{(i)}$, where $L_j^{(i)}$ is the length of the j -th element of link i . The displacement fields can be written in the following matrix form [11]

$$[\bar{u}_{x_j}^{(i)} \ \bar{u}_{y_j}^{(i)} \ \bar{u}_{z_j}^{(i)} \ \bar{\theta}_{x_j}^{(i)}]^T = \mathbf{S}_j^{(i)}(x_j^{(i)}) \mathbf{q}_{f_j}^{(i)} \quad (3)$$

where $\mathbf{S}_j^{(i)}$ is the shape function associated with the j -th element of link i .

Eq. (3) is expressed with respect to the abscissa $x_j^{(i)}$ of the *local* frame of the j -th element of link i . However, to derive the kinetic energy of the flexible link in Section IV. A, Eq. (3) must be expressed with respect to the abscissa x_i of the body-fixed frame $\{i\}$ of link i , see Fig. 4. Therefore

$$[\bar{u}_{x_j}^{(i)} \ \bar{u}_{y_j}^{(i)} \ \bar{u}_{z_j}^{(i)} \ \bar{\theta}_{x_j}^{(i)}]^T = \mathbf{S}_j^{(i)}(x_i - \bar{L}_{j-1}^{(i)}) \mathbf{q}_{f_j}^{(i)}, \quad \bar{L}_j^{(i)} = \sum_{k=1}^j L_k^{(i)} \quad (4)$$

III. NUMBER OF NODES (MARKERS)

To estimate the parameters of a SMS with flexible joints and rigid links, only two encoders at each joint are required, measuring the link and gear motor angular positions q and θ_m , respectively, see Fig. 2, [3]. However, when also considering the manipulator link flexibility, k artificial markers [12], must be attached on link i whose number must be adequate to “observe” the elastic motion of the link.

In this paper, the required number of markers per unit length on link i , i.e. the required *spatial* sampling frequency $f_{s,i}$ of link i , is based on the application of Nyquist’s theorem to the maximum spatial frequency $f_{max,i}$ arising from the dominant eigenmodes of link i

$$f_{s,i} \geq 2f_{max,i} \quad (5)$$

Hence, the required number of markers $N_{s,i}$ for link i is

$$N_{s,i} = f_{s,i} L_i \quad (6)$$

where L_i is the length of link i .

The eigenmodes of each link are obtained using the Euler Bernoulli equations and appropriate boundary conditions, [9]-[11]. In the scope of a multi-link manipulator, the *clamped-loaded* boundary conditions are employed. The clamped assumption is made because the model is derived in the local frame, in which the segment base is always fixed. Furthermore, the loaded assumption at a segment’s endpoint is due to the inertia and mass of the next segments. The detailed procedure can be found in [9]-[11].

Since each link has its base fixed, a marker at this end is not required. Markers placement is assumed to be uniform, i.e. the markers are placed at equal intervals. However, extensive literature exists for sensor placement methods that can be used with the proposed identification method, too. Finally, the last marker is mounted at the link's endpoint.

Since the link is divided into beam elements, the total nodes and thus, the total elements of each link must be determined. In this work, a node is placed at every point with a marker. An additional node is required at the base of the link as it is the first node of the first element. Hence, the number of link i nodes $N_{N,i}$ is equal to the number of markers $N_{s,i}$ required (see Eq. (6)) plus one, and thus, the number of link i elements $N_{el,i}$ will be equal to the number of markers required. Fig. 3 shows the number of nodes and elements of a link for 3 required markers.

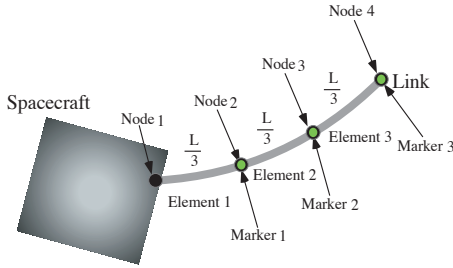


Fig. 3. Number of nodes and elements in the case of 3 required markers.

IV. ENERGY AND DYNAMICS OF FLEXIBLE SPACE MANIPULATOR SYSTEMS

The proposed estimation method is based on the application of the energy balance during the motion of the space manipulator. To derive the system energy, the kinetic and the potential energies of the system have to be computed.

A. Energy of the Flexible Links

The kinetic energy $K_j^{(i)}$ of j -th element of flexible link i consists of the kinetic energy due to the rigid motion induced by motor i and the kinetic energy due to the elastic deformations and is given by

$$K_j^{(i)} = \frac{1}{2} \rho_i A_i \int_{\bar{E}_j^{(i)}}^{\bar{L}_j^{(i)}} \dot{\mathbf{R}}_j^{(i)\top} \dot{\mathbf{R}}_j^{(i)} dx_i \quad (7)$$

where ρ_i , A_i are link's i density and cross-section respectively, and $\mathbf{R}_j^{(i)}$ is the inertial position vector of an arbitrary point along the j -th element of link i , see Fig. 4, given by

$$\mathbf{R}_j^{(i)}(x_i, t) = \mathbf{R}_0 + \mathbf{T}_1^1 \mathbf{r}_j^{(1)}(x_i, t) \quad (8)$$

and

$$\mathbf{R}_j^{(i)}(x_i, t) = \mathbf{R}_j^{(i-1)}(L_{i-1}, t) + \mathbf{T}_i^i \mathbf{r}_j^{(i)}(x_i, t), \quad i=2,3,\dots,N \quad (9)$$

where

$$\mathbf{R}_0 = \mathbf{r}_{0,cm} + \mathbf{T}_0^0 \mathbf{r}_0 \quad (10)$$

where $\mathbf{r}_{0,cm}$ is the position vector of the spacecraft CM, see Fig. 4, ${}^0\mathbf{r}_0$ is the position vector from the spacecraft CM to the first joint expressed in the spacecraft's frame $\{\mathbf{0}\}$, and \mathbf{T}_0 is the rotation matrix between frame $\{\mathbf{0}\}$ and the inertial

frame. The position vector ${}^i\mathbf{r}_j^{(i)}$ of this point with respect to abscissa x_i of body-fixed frame $\{i\}$, is defined by

$${}^i\mathbf{r}_j^{(i)}(x_i) = [x_i + \bar{u}_{x_j}^{(i)}(x_i, t) \quad \bar{u}_{y_j}^{(i)}(x_i, t) \quad \bar{u}_{z_j}^{(i)}(x_i, t)]^T \quad (11)$$

and the cumulative transformation \mathbf{T}_i , $i=1,\dots,N$, between the body-fixed frame $\{i\}$ and the inertial frame, is given by

$$\mathbf{T}_i = \mathbf{T}_{i-1} \mathbf{E}_{i-1} \mathbf{A}_i \quad (12)$$

where $\mathbf{A}_i(q_i)$ is the joint rotation matrix for joint i , q_i is the joint angle after the gearbox, see Fig. 2, and \mathbf{E}_i is the flexible link transformation matrix for link i , given by [13]

$$\mathbf{E}_i = \begin{bmatrix} 1 & -\bar{\theta}_{z_d}^{(i)}(L_i) & \bar{\theta}_{y_d}^{(i)}(L_i) \\ \bar{\theta}_{z_d}^{(i)}(L_i) & 1 & -\bar{\theta}_{x_d}^{(i)}(L_i) \\ -\bar{\theta}_{y_d}^{(i)}(L_i) & \bar{\theta}_{x_d}^{(i)}(L_i) & 1 \end{bmatrix} \quad (13)$$

where subscript d indicates the last element of link i , and $\bar{\theta}_{x_d}^{(i)}(L_i)$, $\bar{\theta}_{y_d}^{(i)}(L_i)$ and $\bar{\theta}_{z_d}^{(i)}(L_i)$ are the x_i , y_i , z_i rotation components of the last element of link i respectively, evaluated at length L_i of link i .

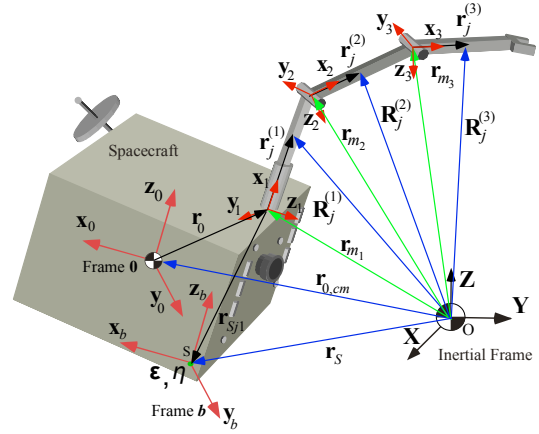


Fig. 4. Position vectors for a flexible link SMS.

The potential energy $U_j^{(i)}$ of the j -th element of the flexible link i is the sum of the torsional strain energy, the longitudinal strain energy and the transverse strain energy

$$U_j^{(i)} = \frac{1}{2} E_i A_i \int_0^{L_i} \left(\frac{\partial \bar{u}_{x_j}^{(i)}(x_i, t)}{\partial x_i} \right)^2 dx_i + \frac{1}{2} (EI_z)_i \int_0^{L_i} \left(\frac{\partial^2 \bar{u}_{z_j}^{(i)}(x_i, t)}{\partial x_i^2} \right)^2 dx_i + \frac{1}{2} (EI_y)_i \int_0^{L_i} \left(\frac{\partial^2 \bar{u}_{y_j}^{(i)}(x_i, t)}{\partial x_i^2} \right)^2 dx_i + \frac{1}{2} (GI_p)_i \int_0^{L_i} \left(\frac{\partial^2 \bar{\theta}_{x_j}^{(i)}(x_i, t)}{\partial x_i^2} \right)^2 dx_i \quad (14)$$

where E_i is the link Young's modulus, and $(EI_y)_i$, $(EI_z)_i$, and $(GI_p)_i$ are the two flexural and the torsional rigidities of link i , respectively.

B. Energy of the Spacecraft

The kinetic energy K_0 of the rigid spacecraft is given by

$$K_0 = \frac{1}{2} m_0 \dot{\mathbf{r}}_{0,cm}^\top \dot{\mathbf{r}}_{0,cm} + \frac{1}{2} \boldsymbol{\omega}_0^\top \mathbf{T}_0^0 \mathbf{I}_0 \mathbf{T}_0^\top \boldsymbol{\omega}_0 \quad (15)$$

where $\dot{\mathbf{r}}_{0,cm}$ is the inertial linear velocity of the spacecraft CM, m_0 is its mass, ${}^0\mathbf{I}_0$ is its moment of inertia with respect to the spacecraft frame $\{\mathbf{0}\}$, and $\boldsymbol{\omega}_0$ is its angular velocity

expressed in the inertial frame. A spacecraft feature point S is tracked, and an observation frame $\{\mathbf{b}\}$ is attached to it, with orientation the same to that of frame $\{\mathbf{0}\}$, see Fig. 4.

The velocity, $\dot{\mathbf{r}}_{0,cm}$ can be calculated according to

$$\dot{\mathbf{r}}_{0,cm} = \dot{\mathbf{r}}_S - \boldsymbol{\omega}_0^\times [\mathbf{T}_0(\boldsymbol{\varepsilon}, \eta)({}^0\mathbf{r}_0 + {}^0\mathbf{r}_{Sy1})] \quad (16)$$

where $\dot{\mathbf{r}}_S$ is the inertial velocity of feature point S, ${}^0\mathbf{r}_{Sy1}$ is the vector from the first joint to point S, $\boldsymbol{\varepsilon}, \eta$ are the Euler parameters which describe the spacecraft attitude, and $(*)^\times$ denotes the cross product matrix of vector $(*)$. The velocity $\dot{\mathbf{r}}_S$ and the Euler parameters $\boldsymbol{\varepsilon}, \eta$ are obtained from measurements. Vector ${}^0\mathbf{r}_{Sy1}$ is known since the location of point S is known and thus, its distance from the first joint is known also. However, the vector ${}^0\mathbf{r}_0$ is considered as unknown, since the spacecraft CM location is considered as an unknown to be estimated by the developed method.

C. Energy of the Flexible Joints

First, the kinetic energy of motor i , see Fig. 2, is given by

$$K_{m_i} = \frac{1}{2} m_{m_i} \dot{\mathbf{r}}_i^T \dot{\mathbf{r}}_i + \frac{1}{2} \boldsymbol{\omega}_{s_i}^T \mathbf{T}_{s_i} {}^s \mathbf{I}_{s_i} \mathbf{T}_{s_i}^T \boldsymbol{\omega}_{s_i} + \frac{1}{2} \boldsymbol{\omega}_{r_i}^T \mathbf{T}_{r_i} {}^r \mathbf{I}_{r_i} \mathbf{T}_{r_i}^T \boldsymbol{\omega}_{r_i} \quad (17)$$

where m_{m_i} is the total mass of the joint's i motor and is the sum of its rotor and stator mass, ${}^s \mathbf{I}_{s_i}$ is the joint's i stator moment of inertia about its local frame $\{s_i\}$ and expressed with respect to this frame, and ${}^r \mathbf{I}_{r_i}$ is the joint's i rotor moment of inertia about its local frame $\{r_i\}$ and expressed with respect to this frame.

The inertial velocity $\dot{\mathbf{r}}_{m_i}$ of the joint's i motor is

$$\dot{\mathbf{r}}_{m_i} = \dot{\mathbf{r}}_S - \dot{\mathbf{T}}_0 {}^0\mathbf{r}_{Sy1} + \sum_{k=1, i>1}^{i-1} [\mathbf{T}_i^k \dot{\mathbf{r}}_i(L_k) + \dot{\mathbf{T}}_i^k \mathbf{r}_i(L_k)] \quad (18)$$

The angular velocity $\boldsymbol{\omega}_{s_i}$ of joint's i stator is

$$\boldsymbol{\omega}_{s_i} = \boldsymbol{\omega}_d^{(i-1)}(L_{i-1}) \quad (19)$$

and the angular velocity $\boldsymbol{\omega}_{r_i}$ of joint's i rotor is

$$\boldsymbol{\omega}_{r_i} = \boldsymbol{\omega}_d^{(i-1)}(L_{i-1}) + n_i \dot{\theta}_{m_i} \mathbf{z}_{m_i} \quad (20)$$

where \mathbf{z}_{m_i} is the unit vector in the direction of joint's i rotor rotation axis and

$$\boldsymbol{\omega}_d^{(i)}(L_i) = \boldsymbol{\omega}_0 + \sum_{k=1}^i \mathbf{T}_k^k \mathbf{z}_k \dot{q}_k + \sum_{k=1, i>1}^i \mathbf{T}_k^k \dot{\boldsymbol{\theta}}_d^{(k)}(L_k) \quad (21)$$

where ${}^i \mathbf{z}_i$ is the unit vector in the direction of joint's i axis expressed in the frame $\{i\}$, and

$$\dot{\boldsymbol{\theta}}_d^{(k)}(L_k) = \begin{bmatrix} \dot{\theta}_{x_d}^{(k)}(L_k) & \dot{\theta}_{y_d}^{(k)}(L_k) & \dot{\theta}_{z_d}^{(k)}(L_k) \end{bmatrix}^T \quad (22)$$

The potential energy due to joint flexibilities and the dissipative losses caused by the damping elements at the joints are given, respectively, by

$$U_m = 1/2 (\boldsymbol{\theta}_m - \mathbf{q})^T \mathbf{K} (\boldsymbol{\theta}_m - \mathbf{q}) \quad (23)$$

and

$$E_{diss} = \int_0^t (\boldsymbol{\theta}_m - \dot{\mathbf{q}})^T \mathbf{B} (\boldsymbol{\theta}_m - \dot{\mathbf{q}}) dt \quad (24)$$

where $\mathbf{K} = \text{diag}(k_1, k_2, \dots, k_N)$, $\mathbf{B} = \text{diag}(b_1, b_2, \dots, b_N)$ and the

column vectors \mathbf{q} and $\boldsymbol{\theta}_m$ define the link and the gear reduction angular positions, respectively

$$\mathbf{q} = [q_1 \ \dots \ q_N]^T, \quad \boldsymbol{\theta}_m = [\theta_{m_1} \ \dots \ \theta_{m_N}]^T \quad (25)$$

where q_i and θ_{m_i} angles are defined in Fig. 2.

D. Dynamics of Flexible Space Manipulator Systems

The system equations of motion are derived using the Lagrangian approach. The system Lagrangian is defined as

$$L = K_{system} - U_{system} \quad (26)$$

and the system total kinetic energy K_{system} and the system total dynamic energy U_{system} are given by

$$K_{system} = K_0 + \sum_{i=1}^N \sum_{j=1}^{N_{el,i}} K_{l_j}^{(i)} + \sum_{i=1}^N K_{m_i} \quad (27)$$

$$U_{system} = \sum_{i=1}^N \sum_{j=1}^{N_{el,i}} U_{l_j}^{(i)} + \sum_{i=1}^N U_{m_i} \quad (28)$$

where $N_{el,i}$ is the number of link's i elements.

The vector of generalized speeds is defined as

$$\mathbf{v} = [\dot{\mathbf{r}}_{0,cm}^T \ \boldsymbol{\omega}_0^T \ \dot{\mathbf{q}}^T \ \dot{\boldsymbol{\theta}}_m^T \ \dot{\mathbf{q}}_f^T]^T \quad (29)$$

where \mathbf{q}_f is the vector that consists of the *global* nodal displacements of all the discretized links and is defined as

$$\mathbf{q}_f = [\mathbf{q}_{f_1}^{(1)T} \ \dots \ \mathbf{q}_{f_{N_{s,1}}}^{(1)T} \ \mathbf{q}_{f_1}^{(2)T} \ \dots \ \mathbf{q}_{f_{N_{s,2}}}^{(2)T} \ \dots \ \mathbf{q}_{f_1}^{(N)T} \ \dots \ \mathbf{q}_{f_{N_{s,N}}}^{(N)T}]_{k \times 1}^T \quad (30)$$

where $k = \sum_{i=1}^N N_{s,i}$ and

$$\mathbf{q}_f^{(i)} = [\mathbf{u}_l^{(i)T} \ \boldsymbol{\theta}_l^{(i)T}]^T \quad (31)$$

where the vectors $\mathbf{u}_l^{(i)}$ and $\boldsymbol{\theta}_l^{(i)}$ that consists of the translations and rotations of node l of link i along and about $x^{(i)}, y^{(i)}, z^{(i)}$ axes respectively, are

$$\mathbf{u}_l^{(i)} = [u_{x_l}^{(i)T} \ u_{y_l}^{(i)T} \ u_{z_l}^{(i)T}]^T, \quad \boldsymbol{\theta}_l^{(i)} = [\theta_{x_l}^{(i)T} \ \theta_{y_l}^{(i)T} \ \theta_{z_l}^{(i)T}]^T \quad (32)$$

Using a Lagrangian approach, the equations of motion are

$$\frac{d}{dt} \left(\frac{\partial L}{\partial \dot{\mathbf{r}}_{0,cm}} \right) - \frac{\partial L}{\partial \mathbf{r}_{0,cm}} = \mathbf{0}_{3 \times 1} \quad (33)$$

$$\frac{d}{dt} \left(\frac{\partial L}{\partial \dot{\boldsymbol{\omega}}_0} \right) + \dot{\mathbf{r}}_{0,cm}^\times \frac{\partial L}{\partial \mathbf{r}_{0,cm}} = \mathbf{0}_{3 \times 1} \quad (34)$$

$$\frac{d}{dt} \left(\frac{\partial L}{\partial \dot{\mathbf{q}}} \right) - \frac{\partial L}{\partial \mathbf{q}} + \frac{\partial D_{diss}}{\partial \dot{\mathbf{q}}} = \mathbf{0}_{N \times 1} \quad (35)$$

$$\frac{d}{dt} \left(\frac{\partial L}{\partial \dot{\boldsymbol{\theta}}_m} \right) - \frac{\partial L}{\partial \boldsymbol{\theta}_m} + \frac{\partial D_{diss}}{\partial \dot{\boldsymbol{\theta}}_m} = \mathbf{n} \boldsymbol{\tau} \quad (36)$$

$$\frac{d}{dt} \left(\frac{\partial L}{\partial \dot{\mathbf{q}}_f} \right) - \frac{\partial L}{\partial \mathbf{q}_f} = \mathbf{0}_{k \times 1} \quad (37)$$

where D_{diss} is a term due to joint damping, given by

$$D_{diss} = 1/2 (\boldsymbol{\theta}_m - \dot{\mathbf{q}})^T \mathbf{B} (\boldsymbol{\theta}_m - \dot{\mathbf{q}}) \quad (38)$$

Also, $\mathbf{n} = \text{diag}(n_1, n_2, \dots, n_N)$, with n_i the i^{th} gear ratio, and $\boldsymbol{\tau}$ is the motor torque column vector given by

$$\boldsymbol{\tau} = [\tau_1 \ \dots \ \tau_N]^\top \quad (39)$$

where τ_i is the i^{th} motor torque.

$$\mathbf{H}\dot{\mathbf{v}} + \mathbf{C} = \mathbf{Q} \quad (40)$$

where \mathbf{H} is the system inertia matrix, the vector \mathbf{C} contains terms due to Coriolis and centrifugal forces, and terms due to the presence of flexibilities. The vector of generalized forces \mathbf{Q} is defined as

$$\mathbf{Q} = [\mathbf{0}_{3 \times 1}^\top \ \mathbf{0}_{3 \times 1}^\top \ \mathbf{0}_{N \times 1}^\top \ (\mathbf{n}\boldsymbol{\tau})^\top \ \mathbf{0}_{k \times 1}^\top]^\top \quad (41)$$

V. PARAMETER ESTIMATION USING THE ENERGY BALANCE

In this section, an estimation method based on the system energy balance is developed. This method does not require acceleration measurements, which contain substantial noise. The method can estimate all parameters required for the system dynamics including those that describe both the joint and link flexibilities.

In free-floating mode, only manipulator joints are active. The energy provided by the joint motors is

$$E_m = \int_0^t \boldsymbol{\tau}^\top \mathbf{n}\dot{\boldsymbol{\theta}}_m dt \quad (42)$$

The energy generated by the motors is balanced by the system kinetic and potential energy and the dissipative losses. Therefore, the energy balance is written as

$$E_m = K_{\text{system}} + U_{\text{system}} + E_{\text{diss}} \quad (43)$$

It can be shown that Eq. (43) can be written in a linear form with respect to the unknown parameters

$$E_m = \mathbf{Y}(\dot{\mathbf{r}}_s, \boldsymbol{\omega}_0, \boldsymbol{\varepsilon}, \boldsymbol{\eta}, \mathbf{q}, \dot{\mathbf{q}}, \boldsymbol{\theta}_m, \dot{\boldsymbol{\theta}}_m, \mathbf{q}_f, \dot{\mathbf{q}}_f) \boldsymbol{\pi} \quad (44)$$

where \mathbf{Y} is the regressor matrix and $\boldsymbol{\pi}$ is the minimal vector of parameters to be estimated which contains all necessary parameters to define the full dynamics of a space manipulator with flexible joints and flexible links. Note that \mathbf{Y} is not a function of accelerations; only readily available positions and velocities measurements are needed to compute it. If n_m measurements of $\dot{\mathbf{r}}_s, \boldsymbol{\omega}_0, \boldsymbol{\varepsilon}, \boldsymbol{\eta}, \mathbf{q}, \dot{\mathbf{q}}, \boldsymbol{\theta}_m, \dot{\boldsymbol{\theta}}_m, \mathbf{q}_f, \dot{\mathbf{q}}_f$ are obtained at given time instants t_1, t_2, \dots, t_{n_m} along an appropriate trajectory, then the following system of equations results

$$\hat{\mathbf{E}}_m^* = \begin{bmatrix} E_m^*(t_1) \\ E_m^*(t_2) \\ \vdots \\ E_m^*(t_{n_m}) \end{bmatrix} = \begin{bmatrix} \mathbf{Y}(t_1) \\ \mathbf{Y}(t_2) \\ \vdots \\ \mathbf{Y}(t_{n_m}) \end{bmatrix} \boldsymbol{\pi} = \hat{\mathbf{Y}} \boldsymbol{\pi} \quad (45)$$

To solve (45) for $\boldsymbol{\pi}$, $\hat{\mathbf{Y}}$ must be of full rank. To avoid ill conditioning of $\hat{\mathbf{Y}}$, the number of measurements should be large enough. The vector of the estimated parameters $\boldsymbol{\pi}$ can be computed by a least-squares technique. All required quantities can be obtained directly or indirectly using available sensors. The required joint angles \mathbf{q} can be obtained directly by link encoders, and $\boldsymbol{\theta}_m$ by joint encoders, while their numerical differentiation provides the rates $\dot{\mathbf{q}}$

and $\dot{\boldsymbol{\theta}}_m$. The orientation of the spacecraft, and thus, the corresponding $\boldsymbol{\varepsilon}, \boldsymbol{\eta}$, are obtained by Star or Sun Trackers, while $\boldsymbol{\omega}_0$ is obtained directly from Inertial Measurement Units (IMUs). The spacecraft linear velocity $\dot{\mathbf{r}}_s$ can be obtained by fusing GNSS, inertial, and magnetometer data, [14]. The elastic displacements \mathbf{q}_f can be measured by link visual sensors, and their rates obtained by differentiation.

VI. SIMULATION RESULTS

The planar space manipulator with two flexible joints and two flexible links shown in Fig. 5 is employed to illustrate the proposed method. The spacecraft parameters are shown in Table I. The motor inertial properties, the properties of the flexible drive as well as the properties of the flexible links are presented in Table II and Table III, respectively. The position vector of S from joint 1 is ${}^0\mathbf{r}_{s/1} = [-1 \ -2]^\top$.

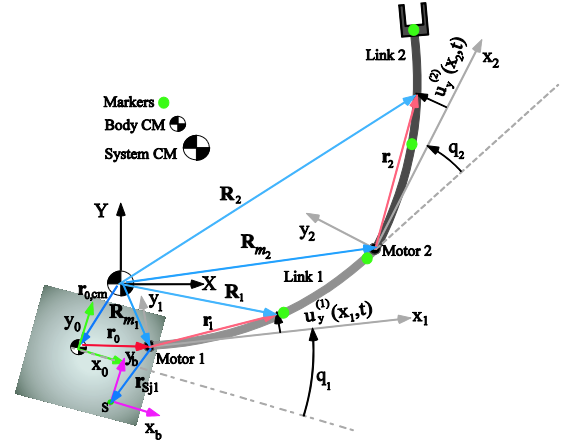


Fig. 5. The planar flexible space manipulator.

TABLE I. PARAMETERS OF THE SPACECRAFT.

Spacecraft	m_0 (kg)	\mathbf{r}_0 (m)	I_{0z} (kg m ²)
	400	$[1 \ 1]^\top$	65

TABLE II. PARAMETERS OF THE MOTORS AND THE DRIVE MECHANISMS.

Motor	n_i	k_i (Nm/rad)	b_i (Nms/rad)	m_{m_i} (kg)	I_{s_i} (kg m ²)	I_{r_i} (kg m ²)
1	50	1000	75.85	3	0.0075	0.0075
2	50	1000	75.85	3	0.0075	0.0075

TABLE III. PARAMETERS OF THE FLEXIBLE LINKS.

Link	$\rho_i A_i$ (kg/m)	$(EI)_i$ (Nm ²)	I_i (kg m ²)	L_i (m)
1	31.42	1768.8	0.1885	1.2
2	31.42	597.87	0.1885	1.2

In this example, bending is considered. It is assumed that the first two eigenmodes sufficiently describe the dominant behavior of the links. The maximum spatial frequencies arising from the dominant eigenmodes of the first and second links are $f_{max,1} = 1.39 \text{ m}^{-1}$ and $f_{max,2} = 1.67 \text{ m}^{-1}$, respectively. Based on Nyquist's theorem and according to Eq. (6), the markers for these links are $N_{s,1} = 2$ and $N_{s,2} = 2$, respectively.

The commanded exciting joint trajectories $q_i^d, i=1,2$ are

$$q_i^d = C_i \sin(\omega_d t) \quad (46)$$

The trajectories parameters were chosen as $\omega_{d,i} = \pi/2$

rad/s, $C_1=1.3$ rad and $C_2=1$ rad. The motion duration is $t_f=10$ s. A PD controller is applied to the system with gains given by $\mathbf{K}_p=\text{diag}(500,500)$ and $\mathbf{K}_D=\text{diag}(100,100)$. The time histories of the joint angles, rates and torques are shown in Fig. 6. The number of measurements taken is $n_m=100$ and the estimated parameters are found solving Eq. (45). The actual and estimated parameter values obtained are displayed in Table V. It can be seen that the method estimates the required parameters successfully.

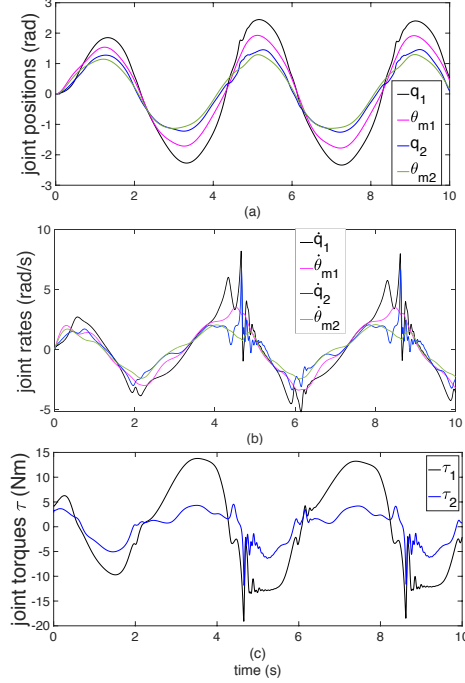


Fig. 6. (a) Manipulator exciting trajectories and inputs. (a) Joint angles \mathbf{q} and θ_m , (b) rates $\dot{\mathbf{q}}$ and $\dot{\theta}_m$, and (c) input torques $\boldsymbol{\tau}$.

TABLE V. ACTUAL AND ESTIMATED PARAMETERS.

π_i	Actual values	Estimated values	Relative error(%)
$I_{0,z}+I_{s1,z}+m_0(r_{0,x}^2+r_{0,y}^2)$ (kg m ²)	865.01	865.02	-0.0014
$m_0 r_{0,x}$ (kg m)	400	400.01	-0.0016
$m_0 r_{0,y}$ (kg m)	400	400.01	-0.0016
$m_0+m_{m_1}$ (kg)	403	403.01	-0.0017
$I_{r1,z}$ (kg m ²)	0.0075	0.0075	-0.0001
$I_{r2,z}$ (kg m ²)	0.0075	0.0075	0.0004
$I_{s2,z}$ (kg m ²)	0.0075	0.0075	0.11
m_{m_2} (kg)	3	3.00	0.0050
$\rho_1 A_1$ (kg/m)	31.42	31.42	-0.0004
$\rho_2 A_2$ (kg/m)	31.42	31.42	0.0002
$(EI_z)_1$ (Nm ²)	1768.8	1768.80	0.0000
$(EI_z)_2$ (Nm ²)	1768.8	1768.80	-0.0016
k_1 (Nm/rad)	1000	1000.00	0.0000
k_2 (Nm/rad)	1000	1000.00	0.0004
b_1 (Nm/rad)	75.85	75.85	0.0002
b_2 (Nm/rad)	75.85	75.85	-0.0008

CONCLUSION

In this paper, the dynamic equations of general space manipulator systems whose manipulators are subject to both link and joint flexibilities were derived. A parameter estimation method, based on the energy balance during manipulator motion, was proposed. The method estimates all system parameters, including those that describe both link and joint flexibilities, and can reconstruct the system full dynamics required for the application of advanced control strategies. The application of the developed method is valid for spatial systems; here it was illustrated by a planar example system.

REFERENCES

- [1] Nanos, K., and Papadopoulos, E., "On the Dynamics and Control of Flexible Joint Space Manipulators," *Control Engineering Practice*, Vol. 45, 2015, pp. 230-243.
- [2] Zou, T., Ni, F., Guo, C., Ma, W., and Liu, H., "Parameter Identification and Controller Design for Flexible Joint of Chinese Space Manipulator," *2014 IEEE International Conference on Robotics and Biomimetics*, Dec., 5-10, Bali, Indonesia, pp. 142-147.
- [3] Nanos, K., and Papadopoulos, E., "On Parameter Estimation of Space Manipulator Systems with Flexible Joints Using the Energy Balance," *IEEE International Conference on Robotics and Automation (ICRA '19)*, Montreal, Canada, May 20-24, 2019, pp. 3570-3576.
- [4] Becedas, J.R. Trapero, H. Sira-Ramirez and V. Feliu-Battle, "Fast identification method to control a flexible manipulator with parameter uncertainties," *IEEE International Conference on Robotics and Automation (ICRA '07)*, Roma, Italy, 10-14 April 2007, pp. 3445-3450.
- [5] Mercere, G., Lovera, M., and Laroche, E., "Identification of a flexible robot manipulator using a linear parameter-varying descriptor state-space structure," *2011 50th IEEE Conference on Decision and Control and European Control Conference (CDC-ECC)*, Orlando, FL, USA, December 12-15, 2011, pp. 818-823.
- [6] Gautier, M., Pham, C.M., and Chedmail, P., "Energy Based Determination of Identifiable Parameters of Flexible Link Robots," *IFAC Robot Control*, Vienna, Austria, 1991, pp. 339-344.
- [7] Behi, F., and Tesar, D., "Parametric Identification for Industrial Manipulators Using Experimental Modal Analysis," *IEEE Transactions on Robotics and Automation*, Vol. 7, No. 5, Oct. 1991, pp. 642-652.
- [8] Xie, Y., Liu, P., and Cai, G.P., "On-orbit identification of flexible parameters of spacecraft," *Proc IMechE, Part K: J Multi-body Dynamics*, 2016; 230: 191-206.
- [9] De Luca, A., and Siciliano, B., "Closed-Form Dynamic Model of Planar Multilink Lightweight Robots," *IEEE Transactions on Systems, Man, and Cybernetics*, Vol. 21, No. 4, 1991, pp. 826-839.
- [10] Shabana, A., *Vibration of discrete and continuous systems*, Springer Science & Business Media, 2012.
- [11] Rognant, M., Courteille, E., and Maurine, P., "Systematic Procedure for the Elastodynamic Modeling and Identification of Robot Manipulators," *IEEE Tr. on Robotics*, v. 26, n. 6, Dec. 2010, pp. 1085-1093.
- [12] Babinec, A, Jurisica, L., Hubinsky, P., and Duchon, F., "Visual Localization of mobile robot using artificial markers," *Procedia Engineering*, Vol. 96, 2004, pp. 1-9.
- [13] Book, W.J., "Recursive Lagrangian Dynamics of Flexible Manipulator Arms," *The Int. J. Robotics Research*, v. 3, n. 3, 1984, pp. 87-101.
- [14] H. F. Grip, T. I. Fossaro, T. A. Johansen, and A. Saberi, "A nonlinear observer for integration of GNSS and IMU measurements with gyro bias estimation," in *Proc. Amer. Contr. Conf.*, 2012, pp. 4607-4612.